Science and Technology Indonesia
e-ISSN:2580-4391 *p*-ISSN:2580-4405
Vol. 9, No. 3, July 2024

Research Paper

High Sensitivity CH_4 and CO_2 Gas Sensor Using Fiber Bragg Grating Coated with Single Layer Graphene

Dedi Irawan[1*], Saktioto[2], Dwi Hanto[3], Bambang Widiyatmoko[3], Sutoyo[4]

[1]*Department of Physics Education, PMIPA, FKIP Universitas Riau, Pekanbaru, 28292, Indonesia*
[2]*Department of Physics, FMIPA, Universitas Riau, Pekanbaru, 28292, Indonesia*
[3]*Research Center for Photonic, National Research and Innovation Agency, BRIN, South Tangerang, 15314, Indonesia*
[4]*Department of Electrical Engineering, UIN Suska Riau, Pekanbaru, 28293, Indonesia*
***Corresponding author**: dedi.irawan@lecturer.unri.ac.id*

Abstract
This article outlines the development of a Fiber Bragg Grating (FBG) intended for use as a sensor for CH_4 and CO_2 gases. Following fabrication, the FBG was effectively treated with a layer of Graphene Material through a modified RF Sputtering process. This coating procedure involved introducing argon gas into the chamber and subjecting the FBG, securely held by two vacuum stages, to a temperature range of 27°C to 600°C by adjusting the power supplied to the cathode and anode, ranging from 0 to 125 Watts. Subsequently, the FBG was employed as a key sensing element within an experimental setup aimed at measuring gas concentrations within a confined space. The assessment involved analyzing the reflected signal of the FBG using an Optical Interrogator System, which demonstrated a shift in the Bragg wavelength of the reflected signal corresponding to varying gas concentrations. This study indicates promising outcomes for the Graphene-coated FBG as a gas sensor. The sensor's sensitivity was evaluated based on the Bragg wavelength shift resulting from gas presence within the chamber. The Graphene-coated FBG exhibited sensitivities of 3.3 ppm for CH_4 and 3.7 ppm for CO_2, surpassing those reported in prior research efforts.

Keywords
Fiber Bragg Grating, Gas Sensor, Graphene, Sensitivity

Received: 18 March 2024, Accepted: 10 June 2024
https://doi.org/10.26554/sti.2024.9.3.710-717

1. INTRODUCTION

In the past twenty years, the adoption of optical technology in both communication and sensor applications has experienced significant and swift expansion (Kersey, 1996; Measures and Abrate, 2002; Yeo et al., 2008). Optical technology offers not just elevated data transfer rates and broader bandwidth, but it also ensures safety by eliminating the need for direct human contact. In communication, optical elements facilitate the transmission, manipulation, and reception of light signals. Similarly, in sensing applications, they enable the detection and assessment of diverse physical parameters. Optical sensor technology finds application across a spectrum of fields, including humidity and temperature sensing, medical diagnostics, aviation, and oil and gas engineering (Jiang, 2022; Shang and Wang, 2021; Stasiewicz et al., 2023; Irawan et al., 2024). Nevertheless, there hasn't been significant progress in the advancement of optical components tailored for gas sensor applications, despite a pressing need for innovation in this domain. Several studies have been conducted to explore relevant technologies in this area. A research Besson et al. (2006) reports the configuration involves designing an acoustic resonance setup employing piezoelectricity and servo electronics. This study quantifies gas concentrations at levels below parts per million (sub-ppm), with the sensitivity highly contingent upon the calibration procedure.

Additional research has documented gas detection techniques utilizing a Spectrometer configuration, comprising a near-infrared tunable fiber laser linked to a sequence of erbium-doped fiber amplifiers, a fiber acoustic sensor, and a primary longitudinal resonance photoacoustic cell. This setup offers the benefits of immunity to electromagnetic interference, safety in flammable and explosive environments, and remote sensing capabilities (Satria et al., 2022). The developed sensor has effectively monitored methane, acetylene, carbon dioxide, carbon monoxide, and water vapor levels in real-time. In fact, this sensor has a detection limit of 87 ppm for CH_4, 1.3 ppm for C_2H_2, 4.6 ppm for CO, 5.5 ppm for CO_2, and 24 ppm for H_2O (Mao et al., 2016).

An alternative approach to gas detection involves utiliz-

ing a sensor featuring a Near-infrared (NIR) distributed feedback (DFB) laser, employing long optical path absorption spectroscopy (Wu et al., 2022). This method was devised to enable the concurrent assessment of atmospheric methane (CH_4), carbon dioxide (CO_2), and oxygen (O_2). Fiber optic switches (FOS) are integrated with time-division multiplexing (TDM) techniques, facilitating the alternating scanning of different lasers across the absorption lines of the target gases. Utilizing long optical path wavelength modulation spectroscopy (WMS) techniques alongside second harmonic detection, as well as employing methods to correct for laser power fluctuations, enhances the precision and accuracy of the sensor. With gas absorption lines selected at 6046.945 cm^{-1}, 6361.245 cm^{-1}, and 7877.647 cm^{-1}, the detection limit (1σ) achieves 0.034 parts per million (ppm) for CH_4, 11.921 ppm for CO_2, and 0.14% for O_2, accounting for concentration and noise levels. Allan deviation analysis demonstrates a 1-second measurement precision of 0.030 ppm for CH4, 11.518 ppm for CO_2, and 0.14% for O_2, with potential enhancements to 0.065 ppm, 0.255 ppm, and 0.005% respectively, with optimal time averaging set at 800 seconds (Munir et al., 2020).

Fiber Bragg Grating (FBG) sensors are pivotal in optical sensing and monitoring across diverse industries. Leveraging fiber optic technology, FBG sensors present numerous merits, rendering them the preferred option for monitoring various physical parameters. Their precise and dependable measurement and monitoring of environmental conditions stand out as a primary rationale for their widespread adoption. Key advantages of FBG sensors encompass their immunity to electromagnetic interference (EMI) and radiation, inherent safety, and capacity to function in challenging environments characterized by high temperatures, pressures, or harsh chemical conditions (Riza et al., 2020).

Another advantage inherent in FBG sensors originates from the fundamental concept of fiber optics. The optical fiber utilized in FBG sensors possesses a low thermal coefficient, enabling operation across a broad temperature spectrum without necessitating additional temperature compensation. Their resistance to corrosion and electromagnetic interference further enhances FBG sensors' suitability for applications demanding high precision and reliability. Additionally, FBG sensors offer benefits in terms of their compact size and light weight. Their relatively diminutive dimensions and minimal mass facilitate seamless integration into structures or equipment without imposing significant additional weight. This adaptability grants flexibility in designing and deploying monitoring systems. Multiplexing represents another pivotal feature that renders FBG sensors highly advantageous. The capability to incorporate multiple FBGs on a single optical fiber facilitates simultaneous monitoring of numerous physical parameters. This not only economizes on expenses but also simplifies the complexity of the monitoring setup. It's noteworthy to underscore that FBG sensors aren't merely passive measuring instruments; they can also serve as actuators. By harnessing the piezoelectric effect in optical fibers, FBG sensors can induce responses or regulate dynamic systems (Yong et al., 2017).

FBG technology has been applied to gas sensing, particularly in the measurement of carbon dioxide (CO_2) concentrations (Song et al., 2024). The investigation focuses on evaluating the accuracy, sensitivity, and response time of sensor readings. The FBG is engineered utilizing a combination of polysulfide (PSF) and polyimide (PI), along with polyethylene glycol (PEG) surfactant, incorporating temperature as a parameter. Findings from this research highlight that the sensitivity of sensor response is influenced by the doping ratio of PI, while PEG surfactant proves effective in reducing the response time for CO_2 sensing. Moreover, the sensitivity and response time of the sensor demonstrate a positive correlation with the thickness of the PSF/PI/PEG CO_2 spectrum layer. Furthermore, the sensor demonstrates the capability to accurately measure CO_2 concentrations within the temperature range of 25–50°C and relative humidity between 35–80%. The proposed sensor exhibits a sensitivity of 3.39 pm/mM, a response time of 310 s, a detection limit of 0.087 mM, a maximum relative error of less than 7.28%, along with high selectivity and durability.

In efforts to boost the sensitivity of the optical fiber sensor, several coating materials have been implemented, including aluminum, gold, silica, and PMMA (Saktioto et al., 2021; Ramadhan et al., 2022). This study aimed to analyze the characteristics of FBG when coated with various materials, focusing on their sensitivity. Results revealed that FBG coated with PMMA exhibited superior sensitivity compared to coatings of aluminum, gold, and silica. Nevertheless, the sensor's stability and durability were compromised as it proved vulnerable to damage from human contact (Qiao et al., 2023; Gao et al., 2021; Wang et al., 2018). By coating the optical fiber with graphene material is a way to enhance the stability and durability (Alberto et al., 2015; Hernaez et al., 2017; Syuhada et al., 2021).

The exceptional properties of graphene offer the potential to enhance both the sensitivity and durability of optical fibers. By applying graphene material onto optical fibers, their resistance to pressure and friction can be significantly increased, owing to graphene's remarkable mechanical strength. Furthermore, graphene's high thermal and electrical conductivity has the capacity to amplify the sensitivity of optical fibers to alterations in temperature and electric fields. Integration of graphene holds promise for the creation of optical sensors that are more responsive and accurate. Utilizing graphene in optical fibers can substantially enhance their performance and resilience, thereby unlocking new possibilities across a range of sensing and optical communication applications (Gao et al., 2021; Yang et al., 2018; Papageorgiou et al., 2017).

In this study, the FBG will undergo a process of layering with graphene material through a modified RF sputtering technique. Subsequently, the measurement system will be employed to assess the sensor component's ability to detect CO_2 and CH_4 gases within a chamber, utilizing the Optical Interrogator System.

2. EXPERIMENTAL SECTION

2.1 Fabrication of FBG

The FBG is produced by employing Silica Single Mode Fiber (SMF) through the Femtosecond laser inscription technique. In this method, extremely short laser pulses induce alterations in the local refractive index within the optical fiber core. The spacing between gratings was maintained at 3 mm. This approach facilitates the creation of periodic gratings with exceptional precision, enabling precise and effective applications in optical sensing for measuring temperature, voltage, or deformation in physical structures (Halstuch and Ishaaya, 2023; Zhou et al., 2003). Throughout the fabrication process, real-time monitoring of the Bragg wavelength, reflection, and transmission signal ratio is conducted via a computer system. The process is programmed to halt automatically upon reaching the preset parameters.

The Bragg wavelength, depicted in Figure 1, represents the peak reflection wavelength generated by the FBG grating.

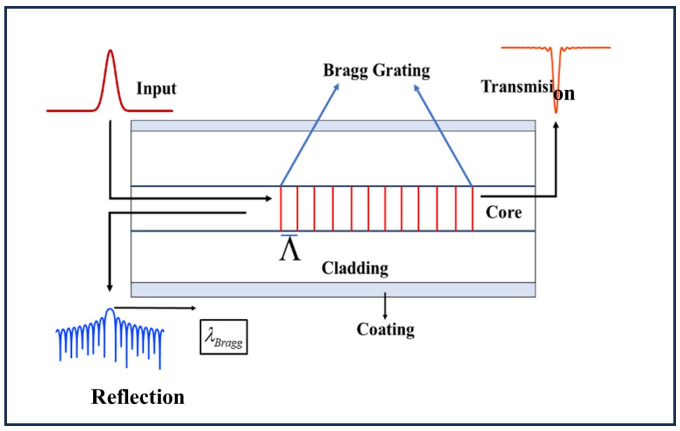

Figure 1. Schematic Diagram of FBG

The peak wavelength undergoes variation in response to parameter alterations such as temperature, stress, strain, pressure, velocity, etc., as expressed mathematically in Equation (1).

$$\lambda_{Bragg} = 2 \wedge n_{eff} \tag{1}$$

Where $\wedge$ is grating length, n_{eff} is effective refractive index, and $\lambda_B ragg$ is Bragg wavelength.

Certain variables impacting the equation include modifications in the effective refractive index of the optical fiber and the sensor's sensitivity to gas detection, as represented by Equation (2).

$$\Delta\lambda_{Bragg} = \frac{d\lambda_{Bragg}}{d\Delta n_{neff}} \Delta n_{eff} = f_{gas}.C_{gas} \tag{2}$$

where $C_g as$ is gas concentration.

The sensitivity of the sensor towards gas detection hinges on how the FBG sensitive layer interacts with a specific gas and the consequent alterations in the effective refractive index. Typically, these equations necessitate experimental calibration to validate the correlation between wavelength changes and gas concentration. It's essential to acknowledge that the attributes of FBG gas sensors can fluctuate based on the sensitive material employed in the FBG layer.

2.2 Coating Process of FBG Surface

The FBG coating procedure was executed utilizing modified RF sputtering, as illustrated in Figure 2. An FBG is positioned on the coating stages, securely held in place by a pair of vacuum holders. The FBG grid is situated in the coating zone just above the substrate, which in this instance is graphene material. The coating process comprises several stages, commencing with cleaning the FBG of contaminants using alcohol, followed by preparation on the sputtering tube. In this scenario, graphene serves as the prepared coating material. Argon gas is introduced into the tube, and heating ensues with a temperature range of 27°C to 600°C, achieved by supplying power to the cathode and anode ranging from 0 to 125 Watts. At a specific temperature, graphene atoms are released and settle on the FBG surface, with the deposition process directed towards the FBG continuing until the desired thickness is achieved. The process concludes with drying and binding. Throughout the coating process, the reflected and transmitted signals are continuously monitored using a power meter to ensure the FBG remains in optimal condition.

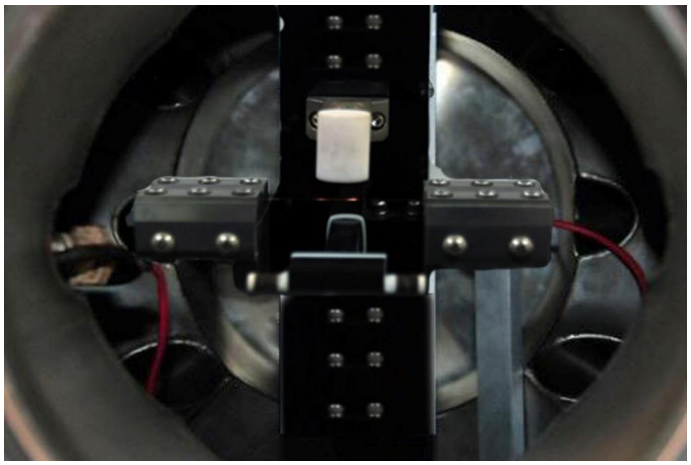

Figure 2. Experimental Set up inside of Sputtering Chamber

2.3 To Analyze the Performance of FBG sensor

Utilizing Graphene on FBG for sensor applications relies on the modulation of the Bragg wavelength. The sensor setup is depicted in Figure 3, where a light source emitting at a wavelength of 1550 nm is coupled through Single Mode Fiber (SMF) to a circulator before reaching the FBG. The FBG is situated within a cylindrical chamber measuring 20 cm in diameter and 30 cm in length. This chamber is equipped with two gas inlets, one for Retaining Gas (CH_4) and the other for Carbon Dioxide

Gas (CO_2). The output signal is then conveyed via SMF to the Optical Spectrum Analyzer (OSA) for further examination of the power spectrum at various wavelengths.

The Bragg grating embedded within the FBG causes a portion of the input signal to be reflected back towards the circulator, which subsequently directs this signal to the sensing analyzer, often referred to as the Optical Interrogator. This Optical Interrogator then displays the reflection signal in real-time as a wavelength-dependent function.

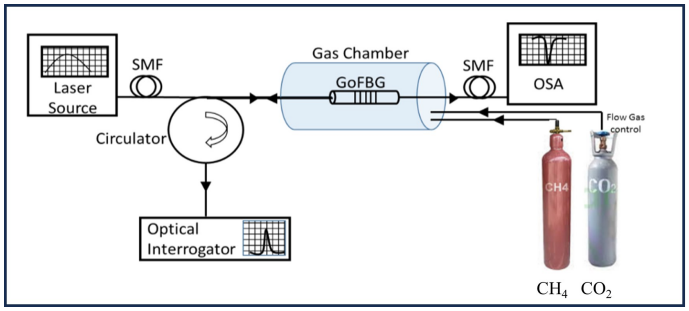

Figure 3. Experimental Set up of CH_4 and CO_2 Gas Sensor System

Optical circulators are employed to steer the flow of light in a designated direction along optical fibers, ensuring the desired transmission of input signals and reflected rays. This directional control simplifies the optical system's design, thereby minimizing its complexity and size, potentially leading to cost savings and enhanced efficiency. Moreover, by segregating input and output lines, these circulators bolster system redundancy and reliability; even if one pathway is disrupted, the remaining lines can operate without interference.

Furthermore, integrating optical interrogators as analyzers for reflected signals is pivotal in this configuration. These interrogators are vital elements within optical sensor systems, responsible for gathering and processing data from optical sensors. Specifically, in the context of monitoring environmental parameters such as atmospheric gas levels, optical interrogators serve as indispensable tools. They swiftly capture and assess this data in real-time, furnishing essential insights for environmental surveillance. Compared to analyzing signals using an Optical Spectrum Analyzer (OSA), leveraging optical interrogators within optical sensor systems offers substantial benefits in terms of precision, speed, and responsiveness. This technological advancement enables optical sensor applications to furnish invaluable data across diverse industries, thereby fostering the continual evolution of optical sensor technology.

3. RESULTS AND DISCUSSION

3.1 Fabricated FBG

A diverse range of fiber Bragg gratings (FBGs) with varying reflection and transmission ratios, spanning from 1% to 99%, has been successfully manufactured. FBGs, which leverage fiber optics, present several advantages that position them as a promising solution for detecting and surveilling gas concentrations across different settings. Their high sensitivity to changes in wavelength enables responsive and precise monitoring capabilities. The utility of FBGs in gas sensors extends beyond merely detecting specific gas concentrations; it extends into broader environmental monitoring contexts. Their capacity to function effectively at elevated temperatures without necessitating additional compensation renders them well-suited for applications within the oil and gas industry.

This study has presented a graphene-coated fiber Bragg grating (FBG) designed for the detection of methane (CH_4) and carbon dioxide (CO_2) gases. The fabrication process achieved success, adhering to the parameters outlined in Table 2.

Table 1. Initial Parameter set up of Coated FBG

Parameters	Value
Core Diameter	8 μm
Core Refractive Index	1.47
Cladding Refractive Index	1.46
Aluminum Refractive index	1.37
PMMA Refractive index	1.49
Graphene Refractive Index	2.7
Chromium(III) Oxide	2.551
Cladding Diameter	125 μm
Graphene layer thickness	0.3 μm
Coating Thickness	20 μm
Peak Wavelength	1550 nm
Grid length	4000 μm
Modulation index	0.0001

3.2 The Graphene Coated FBG

Figure 4 illustrates an FBG comprised of cores and cladding composed of silica single-mode fiber (SMF), essentially forming a grating structure. Subsequently, the SMF FBG undergoes coating with a graphene material layer, approximately 20 micrometers thick. The diagram depicts the geometric arrangement of the graphene-coated FBG, encompassing cores, cladding, grating, graphene coating, and enclosures.

The application of modified RF sputtering was employed for the coating process, depositing graphene material onto the surface of the FBG, thereby influencing its optical properties. Figure 5 clearly illustrates the spectrum of the reflected signal for each apodization profile (Tanh, Uniform, and Gaussian) on the FBG coated with a single layer of graphene material. The Gaussian apodization notably reduced the peak of the reflected signal to a greater extent compared to Uniform apodization. Although apodization can narrow the Full-width Half Maximum (FWHM), the distinction lies in the main lobe and side lobe of the FBG sensor. Gaussian apodization exhibited significant differences in both the main lobe and side lobe compared to Uniform apodization, with a variance of 1.3 nm. Conversely, Uniform apodization demonstrated variances of 3,732 nm.

Table 2. Comparison between Propose Study with Previous Results

Inventor	Gas type	Material Sensor	Sensitivity
(Shen et al., 2021)	CO_2	Polymer Nanocomposite	3 ppm
(Zhao et al., 2022)	CH_4	Carbon Nanostructure	2.2 ppm
(Abdali et al., 2019)	CO_2	Amino-functionalized graphene (AmG)/polyaniline (PANI)/poly(methyl methacrylate) (PMMA) nanofiber	1.7 ppm
(Zhang et al., 2016)	CH_4	Nanostructured Material	1 ppm
(Huang et al., 2003)	CO_2	Polyaniline nanofibers	1 ppm
(Ameloot et al., 2011)	CO_2	Metal-organic frameworks (MOFs)	2.4 ppm (below 5 ppm)
This propose study	CH_4	Graphene Coated FBG	3.3 ppm
This propose study	CO_2	Graphene Coated FBG	3.7 ppm

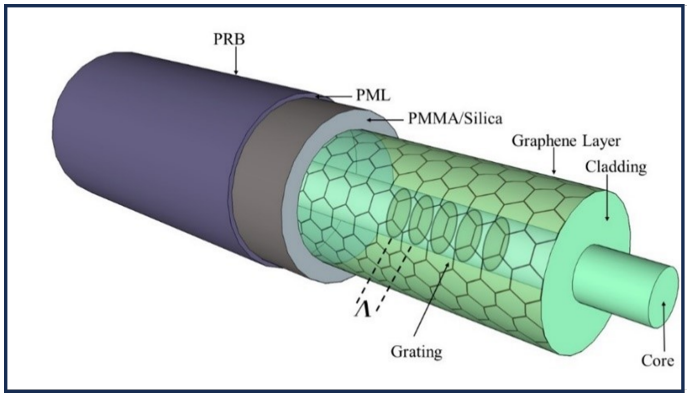

Figure 4. Graphene-Coated FBG for CH_4 and CO_2 Gas Sensor Application

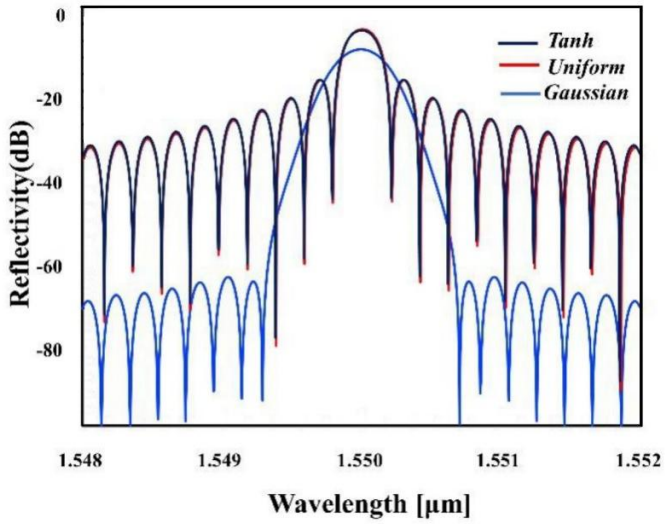

Figure 5. FBG Coating Reflection Spectrum with Different Apodization Grating Structure

These disparities in the main lobe and large side lobe suggest enhanced and precise performance of the FBG sensor, facilitating easier interpretation of the obtained reflections. Apodization significantly influences the grating structure of the FBG, narrowing the FWHM in the resulting reflection spectrum. This enhancement in spectrum resolution through apodization augments the accuracy of the resulting spectrum, as depicted in Figure 5. The apodization function directly correlates with the effective refractive index derived from the coated FBG.

The disparities in the positioning of the main lobe and side lobes within the graphene-coated FBG gas sensor, as observed in the reflection spectrum, directly influence the accuracy and sensitivity of the sensor. Optimal sensor performance is distinguished by substantial discrepancies between the lobes and side lobes. The discrepancy in the main lobe and side lobe of Gaussian apodization is the most pronounced among the various apodizations, with a categorized difference of 0.956 nm, followed by Tanh apodization at 0.508 nm and Uniform at 0.3 nm. Additionally, the analysis of ripple factor indicates that apodization minimizes the ripple factor compared to Uniform apodization.

The graphene-coated Silica SMF FBG, featuring a 20-micrometer-thick graphene layer, exhibits transmission and reflection spectra, as depicted in Figure 6. A FBG design comprising a Silica core and cladding, with a coating layer of PMMA, showcases its transmission and reflection spectra. The FBG structure comprises a core and cladding of Silica material, with a coating layer having a refractive index of 1.5. The transmission spectrum is represented by Figure 6(a), while Figure 6(b) illustrates the reflection spectrum.

The application potential of FBG continues to expand, with its efficacy hinging not only on the fundamental FBG structure but also on the sensitive layer overlaid onto the FBG grating. The judicious selection of sensitive materials stands as a crucial parameter in enhancing sensor selectivity towards specific gases. Innovations in sensitive materials, including the incorporation of nanomaterials or functionalization with specialized compounds, offer avenues for enhancing sensor responsiveness and selectivity.

The benefits of FBG multiplexing enable the deployment of multiple gas sensors on a single optical fiber, optimizing

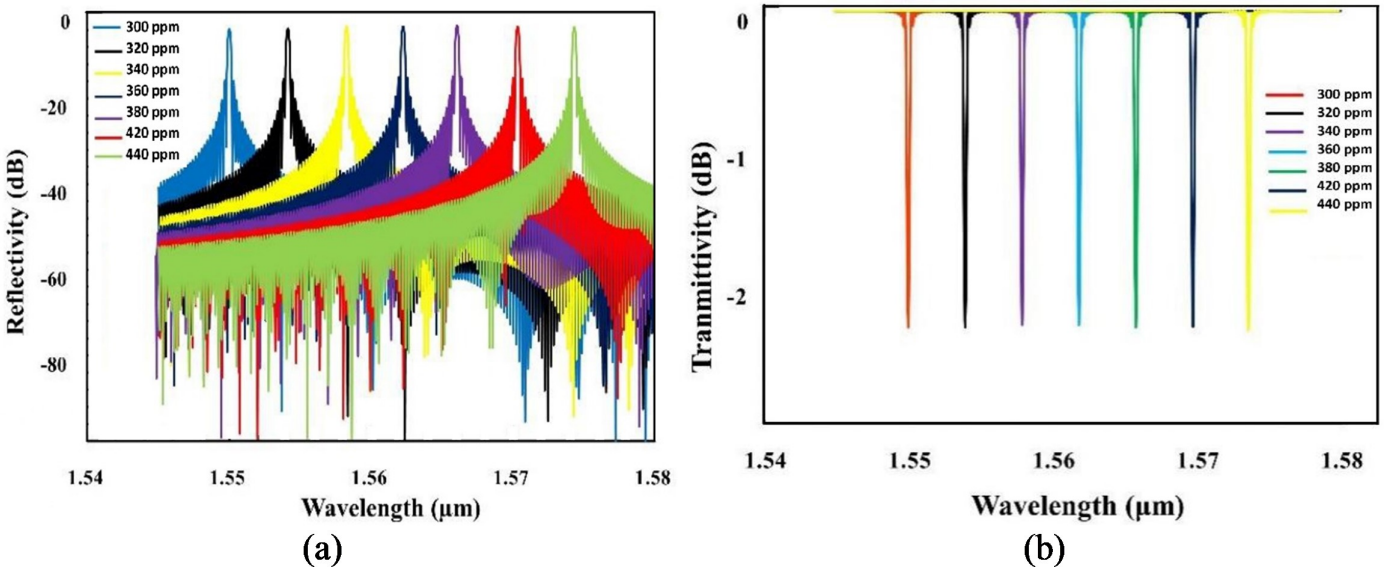

Figure 6. (a) FBG PMMA Reflectivity, (b) FBG PMMA Transmittivity Spectrum

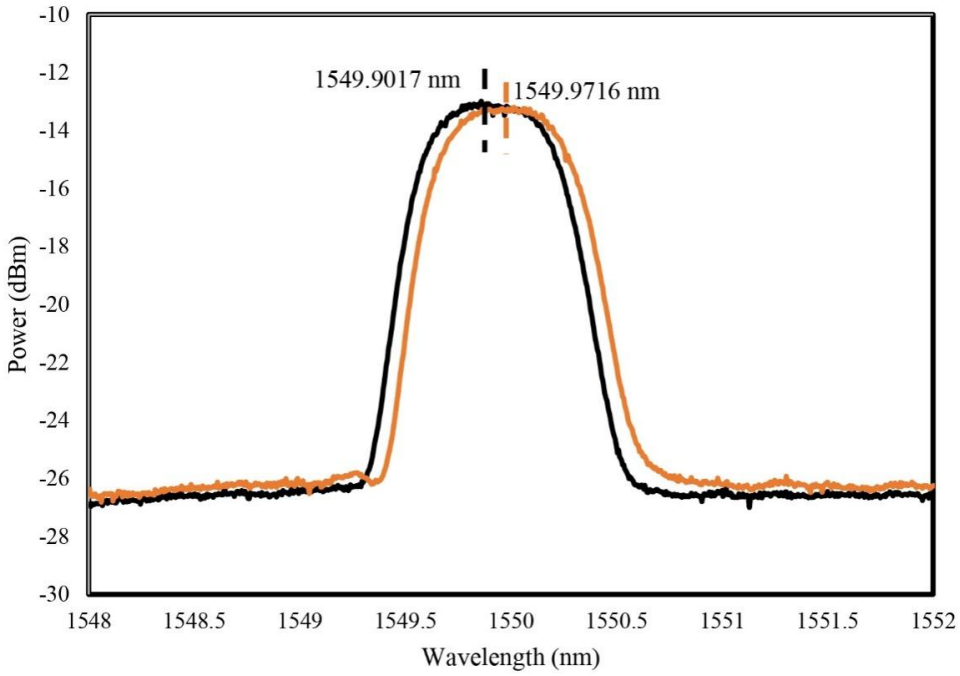

Figure 7. The Spectrums of Reflected Signal of FBG for Difference Gas Concentration Measurement by Optical Interrogator System

resource utilization and reducing installation expenses. This confers the flexibility and efficiency necessary for gas monitoring in intricate industrial settings. Furthermore, the integration of FBG into centralized monitoring systems yields additional advantages in the comprehensive management and interpretation of data.

While FBG presents numerous advantages, its utilization in gas sensors is not devoid of challenges. Ongoing research and development are imperative for the proper selection of sensitive materials and a comprehensive understanding of the properties of the gases being measured. A meticulous calibration process is essential to ensure the FBG gas sensor delivers accurate and consistent responses.

The emergence of FBG-based gas sensor concepts has spurred further innovation. Integrating nanotechnology-based materials into sensitive coatings or combining FBG with other

technologies holds promise for enhancing sensor sensitivity and reliability. In prospective scenarios, FBG applications could extend to monitoring gases in urban environments, facilitating more precise air quality measurements and furnishing invaluable data for environmental policymaking.

3.3 Sensor Sensitivity

In summary, the incorporation of FBG into gas sensors not only addresses the detection of hazardous gases but also facilitates a more comprehensive approach to environmental monitoring. Its inherent safety, heightened sensitivity, and adaptable design render FBG a promising option for realizing advanced and dependable gas monitoring systems. The measurement process, as depicted in Figure 3, involves pumping gas into the chamber, followed by comparing specific conditions with an ideal reference, ultimately yielding a spectrum of Bragg wavelengths, as illustrated in Figure 7.

The Bragg wavelengths of these two signals are determined to be 1549.9017 nm and 1549.9716 nm. This resultant wavelength shift of 0.07 nm is subsequently formulated into a gas concentration of 3.3 ppm for CH_4 gas. Likewise, the sensitivity of the proposed sensor for CO_2 gas is calculated to be 3.7 mm, surpassing the performance of previous studies, as demonstrated in Table 2.

The mean Bragg wavelength under ideal conditions is determined to be 1549.9017 nm after measuring fresh air for approximately 2-3 hours. Additionally, with the precise chamber volume established, the gas concentration within the chamber can be computed utilizing a gas flow meter. For comparison and calibration of gas concentration within the chamber, a conventional CO_2 and CH_4 gas detector were also employed. Utilizing coated FBG for gas concentration detection involved conducting various measurements for both CO_2 and CH_4 gases.

4. CONCLUSIONS

The utilization of Fiber Bragg Grating (FBG) as a gas sensor presents significant promise in gas monitoring and detection endeavors. FBG demonstrates the capability to accurately and promptly detect gas concentrations with heightened sensitivity, facilitated by alterations in the Bragg wavelength. This study introduces a sensor element comprising FBG coated with graphene material, along with an experimental setup tailored for measuring gas concentration using a sensor interrogator system. By measuring the reflected signal, the shift in Bragg wavelength is determined and subsequently converted into sensor sensitivity. For the proposed design, sensitivities of 3.3 ppm and 3.7 ppm are attained for CH_4 and CO_2 gases, respectively.

5. ACKNOWLEDGMENT

We extend our gratitude to LPPM Universitas Riau and BRIN Kemdikbud Ristek for their invaluable support in this research, facilitated through the BRIN-RIIM research with Contract No. 16315/UN19.5.1.3/AL.04/2023.

REFERENCES

Abdali, H., B. Heli, and A. Ajji (2019). Stable and Sensitive Amino-Functionalized Graphene/Polyaniline Nanofiber Composites for Room-Temperature Carbon Dioxide Sensing. *RSC Advances*, **9**(70); 41240–41247

Alberto, N., C. Vigario, D. Duarte, N. A. F. Almeida, G. Gonçalves, J. L. Pinto, P. A. A. P. Marques, R. Nogueira, and V. Neto (2015). Characterization of Graphene Oxide Coatings onto Optical Fibers for Sensing Applications. *Materials Today: Proceedings*, **2**(1); 171–177

Ameloot, R., F. Vermoortele, W. Vanhove, M. B. J. Roeffaers, B. F. Sels, and D. E. De Vos (2011). Interfacial Synthesis of Hollow Metal-Organic Framework Capsules Demonstrating Selective Permeability. *Nature Chemistry*, **3**(5); 382–387

Besson, J.-P., S. Schilt, and L. Thévenaz (2006). Sub-Ppm Multi-Gas Photoacoustic Sensor. *Spectrochimica Acta Part A: Molecular and Biomolecular Spectroscopy*, **63**(5); 899–904

Gao, X. G., L. X. Cheng, W. S. Jiang, X. K. Li, and F. Xing (2021). Graphene and Its Derivatives-Based Optical Sensors. *Frontiers in Chemistry*, **9**; 615164

Halstuch, A. and A. A. Ishaaya (2023). Femtosecond Inscription of a Fiber Bragg Grating Spectral Array in the Same Spatial Location. *Sensors*, **8**; 4064

Hernaez, M., C. R. Zamarreño, S. Melendi-Espina, L. R. Bird, A. G. Mayes, and F. J. Arregui (2017). Optical Fibre Sensors Using Graphene-Based Materials: A Review. *Sensors (Switzerland)*, **17**(1); 155

Huang, J., S. Virji, B. H. Weiller, and R. B. Kaner (2003). Polyaniline Nanofibers: Facile Synthesis and Chemical Sensors. *Journal of the American Chemical Society*, **125**(2); 314–315.

Irawan, D., Azhar, K. Ramadhan, A. Marwin, and A. Marwan (2024). Numerical Study of Early Detection of Tuberculosis Infected with High Sensitivity Plasmonic Sensor. *Science and Technology Indonesia*, **9**(1); 94–102

Jiang, Y. (2022). Application of Optical Fiber Sensing Technology in Bridge Detection. *Highlights in Science, Engineering and Technology*, **9**; 111–114

Kersey, A. D. (1996). A Review of Recent Developments in Fiber Optic Sensor Technology. *Optical Fiber Technology*, **2**(3); 291–317

Mao, X., X. Zhou, Z. Gong, and Q. Yu (2016). An All-Optical Photoacoustic Spectrometer for Multi-Gas Analysis. *Sensors and Actuators B: Chemical*, **232**; 251–256

Measures, R. and S. Abrate (2002). Structural Monitoring with Fiber Optic Technology. *Applied Mechanics Reviews*, **5**(1); 10

Munir, M. A., K. H. Badri, L. Y. Heng, and S. Ibrahim (2020). Biogenic Amines Detection by Chromatography and Sensor Methods: A Comparative Review. *Science and Technology Indonesia*, **5**(4); 90–110

Papageorgiou, D. G., I. A. Kinloch, and R. J. Young (2017). Mechanical Properties of Graphene and Graphene-Based Nanocomposites. *Progress in Materials Science*, **90**; 75–127

Qiao, H., Z. Lin, X. Sun, W. Li, Y. Zhao, and C. Guo (2023).

Fiber Optic-Based Durability Monitoring in Smart Concrete: A State-of-Art Review. *Sensors*, **23**(18); 7810

Ramadhan, K., D. Irawan, and A. Azhar (2022). Optimum Design Sapphire-Fiber Bragg Grating for High-Temperature Sensing. *Jurnal Penelitian Pendidikan IPA*, **8**(3); 1361–1367

Riza, M. A., Y. I. Go, S. W. Harun, and R. R. J. Maier (2020). FBG Sensors for Environmental and Biochemical Applications - A Review. *IEEE Sensors Journal*, **20**(14); 7614–7627

Saktioto, T., K. Ramadhan, Y. Soerbakti, R. F. Syahputra, D. Irawan, and Okfalisa (2021). Apodization Sensor Performance for TOPAS Fiber Bragg Grating. *Telkomnika (Telecommunication Computing Electronics and Control)*, **19**(6); 1982–1991

Satria, E., M. Febrina, M. Djamal, W. Srigutomo, and M. Liess (2022). CO_2 Thermal Conductivity Detection in Gas Mixture for Concentration Measurement Using Bridge Configuration of Thermopiles. *Science and Technology Indonesia*, **7**(4); 443–448

Shang, Y. and C. Wang (2021). Review of Distributed Optical Fiber Sensing Technology. *Yingyong Kexue Xuebao/Journal of Applied Sciences*, **39**(5); 843–857

Shen, B., F. Zhang, L. Jiang, X. Liu, X. Song, X. Qin, and X. Li (2021). Improved Sensing Properties of Thermal Conductivity-Type CO_2 Gas Sensors by Loading Multi-Walled Carbon Nanotubes into Nano-Al_2O_3 Powders. *Frontiers in Energy Research*, **9**; 1–11

Song, S., L. Li, J. Chen, N. Zhong, Y. Liu, Y. He, H. Chang, B. Wan, D. Zhong, Y. Liu, and Q. Xie (2024). Fiber Bragg Grating Sensor for Accurate and Sensitive Detection of Carbon Dioxide Concentration. *Sensors and Actuators B: Chemical*, **404**; 135264

Stasiewicz, K. A., I. Jakubowska, J. Moś, R. Kosturek, and K. Kowiorski (2023). In-Line Gas Sensor Based on the Optical Fiber Taper Technology with a Graphene Oxide Layer. *Electronics (Switzerland)*, **12**(4); 830

Syuhada, A., M. S. Shamsudin, S. Daud, G. Krishnan, S. W. Harun, and M. S. A. Aziz (2021). Single-Mode Modified Tapered Fiber Structure Functionalized with GO-PVA Composite Layer for Relative Humidity Sensing. *Photonic Sensors*, **11**; 314–324

Wang, H., L. Jiang, and P. Xiang (2018). Improving the Durability of the Optical Fiber Sensor Based on Strain Transfer Analysis. *Optical Fiber Technology*, **42**; 97–104

Wu, X., Y. Du, S. Shi, C. Jiang, X. Deng, S. Zhu, X. Jin, and J. Li (2022). Simultaneous Detection of CO_2 and CH_4 Using a DFB Diode Laser-Based Absorption Spectrometer. *Chemosensors*, **10**(10); 390

Yang, Y., J. Sun, L. Liu, S. Zhu, and X. Yuan (2018). Research of Detection Depth for Graphene-Based Optical Sensor. *Optics Communications*, **411**; 143–147.

Yeo, T. L., T. Sun, and K. T. V. Grattan (2008). Fibre-Optic Sensor Technologies for Humidity and Moisture Measurement. *Sensors and Actuators, A: Physical*, **144**(2); 280–295

Yong, Y.-T., S.-C. Lee, and F. A. Rahman (2017). Fiber Sensor Network with Multipoint Sensing Using Double-Pass Hybrid LPFG-FBG Sensor Configuration. *Optics Communications*, **387**; 191–195

Zhang, J., X. Liu, G. Neri, and N. Pinna (2016). Nanostructured Materials for Room-Temperature Gas Sensors. *Advanced Materials*, **28**(5); 795–831

Zhao, W., N. Alcheikh, S. B. Mbarek, and M. I. Younis (2022). Multi-Functional Resonant Micro-Sensor for Simultaneous Magnetic, CO_2, and CH_4 Detection. *Journal of Applied Physics*, **132**(14); 144502

Zhou, Z., T. Graver, L. Hsu, and J. Ou (2003). Techniques of Advanced FBG Sensors: Fabrication, Demodulation, Encapsulation, and Their Application in the Structural Health Monitoring of Bridges. *Pacific Science Review*, **5**(1); 116–121

